ISSN 0003-6838, Applied Biochemistry and Microbiology, 2024, Vol. 60, No. 6, pp. 1118–1130. © Pleiades Publishing, Inc., 2024.
ISSN 0003-6838, Applied Biochemistry and Microbiology, 2024. © Pleiades Publishing, Inc., 2024.

# New 4-styrylcoumarin Derivatives as Potentials Fluorescent Labels for Biomolecules: Application in RNA-fish Probes

**R. Eustáquio[a], A. T. Caldeira[a, b, c], S. Arantes[a], A. Candeias[a, b, c], and A. Pereira[a, b, *]**

[a] *HERCULES Laboratory, IN2PAST—Associate Laboratory for Research and Inno-vation in Heritage, Arts, Sustainability and Territory, University of Évora, Évora, 7000-809 Portugal*

[b] *Department of Chemistry and Biochemistry, School of Sciences and Technology, University of Évora, Évora, 7000-671 Portugal*

[c] *City U Macau Chair in Sustainable Heritage, Sino-Portugal Joint Laboratory of Cultural Heritage Conservation Science, University of Évora, Évora, 7000-809 Portugal*

**e-mail: amlp@uevora.pt*

Received October 18, 2023; revised June 25, 2024; accepted July 3, 2024

**Abstract**—Fluorescence microscopy is a highly sensitive imaging technique used in various scientific fields such as cellular biology, environmental sciences, medicine, and pharmacy. It offers the advantage of using multiple fluorescent labels to visualize different biomolecules and generate multicolored images for identifying specific components within complex biomolecular structures and studying their interactions. These fluorescent labels create chemically stable and minimally disruptive bioconjugates. Amino-reactive fluorescent labels, due to their ease of incorporation into biomolecules, are commonly used in applications like fluorescence in situ hybridization, histochemistry, cell tracing, receptor binding, and immunochemistry. However, the existing popular fluorescent labels are expensive, making coumarin derivatives a potential cost-effective solution for developing bright fluorophores. In this study, the fluorescent 4-styrylcoumarin derivative labels were synthesized and evaluated as potentially effective fluorescent labels for biomolecules. Twelve new fluorescent oligonucleotide probes have been obtained, 6 directed to the rRNA region of eukaryotic cells (EUK516) and 6 directed to the rRNA region of prokaryotic cells (EUB338). The developed fluorescent probes were tested on microorganisms belonging to the culture collection of the Laboratory of Biodegradation and Biotechnology of the HERCULES Laboratory (University of Évora, Portugal), showing effective performance as RNA-FISH probes. These findings evidenced the applicability of the new 4-styrylcoumarin derivatives in labeling of biomolecules and bioimaging.

**Keywords:** fluorescent labels, 4-styrylcoumarin derivatives, biomolecules, RNA-FISH probes

**DOI:** 10.1134/S000368382360286X

Fluorescence microscopy stands as a remarkably sensitive imaging method, enabling the identification, visualization, and monitoring of biomolecules in various critical scientific domains, including but not limited to medicine, pharmaceuticals, cellular biology, and environmental sciences [1–5]. This method provides a significant benefit: the capacity to utilize numerous fluorescent markers for identifying various biomolecules, resulting in the creation of multicoloured images that enhance the accurate discernment of individual components within complex biomolecular structures, both in vitro and in vivo. Additionally, fluorescence microscopy empowers the investigation of their interactions [1, 6–8].

Furthermore, the utilization of fluorescent markers offers several advantages, taking into consideration the remarkable sensitivity and non-invasive nature of the fluorescence technique. Among these benefits are the ability to work with minimal sample quantities and the availability of specific fluorescent label [9]. These fluorescent labels can generate chemically stable, small-sized bioconjugates that have minimal impact on the structure and biological functions of the unlabeled biomolecules [10]. Notably, amine-reactive fluorescent labels, owing to the abundance of amino groups and their ease of integration into biomolecules, are commonly employed for the preparation of bioconjugates in various biological applications, including histochemistry, cell tracing, receptor binding, direct and indirect immunochemistry, and fluorescence in situ hybridization (FISH) [11–13].

Of all the biological applications mentioned above, FISH emerges as a pivotal method employed for the precise spatial detection and quantification of nucleic acids within their cellular context. FISH emerged as a development from non-fluorescent in situ hybridization (ISH). The original ISH technique, initially documented in 1969, relied on staining principles rooted in the complementary pairing of a nucleotide probe, labeled with a reporter molecule, with a distinct target

nucleic acid sequence found within cellular compartments [14, 15]. In 1980, the first application of FISH was described for the specific binding of DNA, employing 3'-fluorescence-tagged RNA probe [16, 17]. FISH enables the recognition of microbial target organisms, such as bacteria, yeasts, and protozoa, at the genus or species level. This is achieved by employing short oligonucleotide probes, typically from 18 to 25 base pairs in size and labeled with fluorescence, which specifically bind to ribosomal RNA. Subsequent analysis was carried out under a fluorescence microscope. Fluorescently labeling oligonucleotide probes present several advantages. These include the capability to directly visualize results without the need for additional detection steps, maintaining an acceptably low background fluorescence, and facilitating the possibility of conducting multicolor detections [18].

Presently, the fluorescent labels most employed are characterized by their high cost, and some of them exhibit small Stokes shifts, often less than 30 nm (such as fluorescein, rhodamine, oxazine, and cyanine). Consequently, coumarin derivatives emerge as a promising solution for the development of economical yet highly luminescent fluorophores featuring substantial Stokes shifts [19, 20]. Coumarins, in addition to their notable biological activity, [21, 22] constitute a primary category of fluorescent dyes extensively utilized across various applications [22–28].

In this study, we intend to evaluate the fluorescent 4-styrylcoumarin derivative labels we've synthesized, through a cost-effective and efficient synthetic approach, as potentially effective fluorescent labels for biomolecules. The new fluorescent oligonucleotide probes, 6 directed to the rRNA region of eukaryotic cells (EUK516) and 6 directed to the rRNA region of prokaryotic cells (EUB338) will be tested on microorganisms belonging to the culture collection of the Laboratory of Biodegradation and Biotechnology of the HERCULES Laboratory (University of Évora, Portugal).

## MATERIALS AND METHODS

**Chemicals, nucleotides and buffers.** The oligonucleotides, EUK516-mod (5'-ACCAGACTTGCCCTCC-3') and EUB338-mod (5'-GCTGCCTCCCGTAGGAGT-3') amino-modified 5'-AC6 targeting the rRNA regions of eukaryotic (yeast) and prokaryotic (bacteria) cells, respectively, were acquired from Eurofins Scientific and STAB Vida (Portugal). Prior to the reaction with these amine-modified oligonucleotides, the reactive dye was dissolved in anhydrous dimethylsulfoxide (DMSO). The developed fluorescent probes were tested on microorganisms belonging to the culture collection of the Laboratory of Biodegradation and Biotechnology of the HERCULES Laboratory (University of Évora, Portugal), namely *Saccharomyces cerevisiae* and *Bacillus* sp. For this purpose, *S. cerevisiae* and *Bacillus* cells were grown at 30°C in malt extract liquid medium (Malt Extract Broth, Himedia, India) for 48 h and nutrient broth (NB) for 24 h, respectively.

The universal probes EUB338-Cy3-(5'Cy3-GCTGCCTCCCGTAGGAGT-3') and EUK516-Cy3-(5'Cy3- ACCAGACTTGCCCTCC-3') targeting the RNAr regions of prokaryotic (bacteria) and eukaryotic (yeast) cells, respectively, were used for hybridization control. These probes have as fluorescent label cyanine (Cy3) bound to the 5' end of the oligonucleotide. The phosphate-buffered saline (PBS 10×) (130.0 mM NaCl, 8.0 mM $NaH_2PO_4$, 2.7 mM KCl, and 1.5 mM $KH_2PO_4$, at a pH of 7.2) and hybridization buffer (HB) (NaCl 0.9 M, Tris-HCl 20 mM, SDS 0.1%) required for the FISH technique procedure were previously prepared.

**Synthesis of (*E*)-2,5-dioxopyrrolidin-1-il-6-(4-(2-(2-(dicyanomethylene)-7-(diethylamino)-2*H*-chromen-4-yl)vinyl)phenoxy)hexanoate (1).** The synthesis of (*E*)-2,5-dioxopyrrolidin-1-il-6-(4-(2-(2-(dicyanomethylene)-7-(diethylamino)-2*H*-chromen-4-il)vinyl)phenoxy)hexanoate (**1**) was conducted in accordance with the methodology described by Eustáquio et al. [29].

**Synthesis of (*E*)-2,5-dioxopyrrolidin-1-yl-6-((4-(2-(2-(dicyanomethylene)-7-(diethylamino)-2*H*-chromen-4-yl)vinyl)phenyl)(methyl)amino)hexanoate (2).** The synthesis of (*E*)-2,5-dioxopyrrolidin-1-yl-6-((4-(2-(2-(dicyanomethylene)-7-(diethylamino)-2*H*-chromen-4-yl)vinyl)phenyl)(methyl)amino)hexanoate (**2**) was conducted in accordance with the method described by Eustáquio et al. [30].

**Synthesis of 4-(cyano((*E*)-7-(diethylamino)-4-((*E*)-4-((6-((2,5-dioxopyrrolidin-1-yl)oxy)-6-oxohexyl)oxy)styryl)-2*H*-chromen-2-ylidene)methyl)-1-methylpyridin-1-ium iodide (3).** The synthesis of 4-(cyano((*E*)-7-(diethylamino)-4-((*E*)-4-((6-((2,5-dioxopyrrolidin-1-yl)oxy)-6-oxohexyl)oxy)styryl)-2*H*-chromen-2-ylidene)methyl)-1-methylpyridin-1-ium iodide (**3**) was conducted in accordance with the methodology performed by Eustáquio et al. [30].

**Synthesis of 4-(cyano((*E*)-7-(diethylamino)-4-((*E*)-4-((6-((2,5-dioxopyrrolidin-1-yl)oxy)-6-oxohexyl)-(methyl)amino)styryl)-2*H*-chromen-2-ylidene)methyl)-1-methyl-pyridin-1-ium iodide (4).** The synthesis of 4-(cyano((*E*)-7-(diethylamino)-4-((*E*)-4-((6-((2,5-dioxopyrrolidin-1-yl)oxy)-6-oxohexyl)(methyl)amino) styryl)-2*H*-chromen-2-yli-dene)methyl)-1-methyl-pyridin-1-ium iodide (**4**) was conducted in accordance with the method described by Eustáquio et al. [30].

**Synthesis of (*E*)-1-(7-(diethylamino)-4-(4-((6-((2,5-dioxopyrrolidin-1-yl)oxy)-6-oxohexyl)oxy)styryl)-2*H*-chromen-2-ylidene)piperidin-1-ium nitrate (5).** Synthesis of (*E*)-1-(7-(diethylamino)-4-(4-((6-((2,5-dioxopyrrolidin-1-yl)oxy)-6-oxohexyl)oxy)styryl)-2*H*-chromen-2-ylidene)piperidin-1-ium nitrate (**5**) was conducted in accordance with the methodology performed by Eustáquio et al. [31].

**Synthesis of (*E*)-1-(7-(diethylamino)-4-(4-((6-((2,5-dioxopyrrolidin-1-yl)oxy)-6-oxohexyl)(methyl)-amino)styryl)-2*H*-chromen-2-ylidene)piperidin-1-ium nitrate (6).** The synthesis of (*E*)-1-(7-(diethylamino)-4-(4-((6-((2,5-dioxopyrrolidin-1-yl)oxy)-6-oxohexyl)-(methyl)amino)styryl)-2*H*-chromen-2-ylide-ne)piperidin-1-ium nitrate (**6**) was conducted in accordance with the method described by Eustáquio et al. [30].

**Labeling of amino-modified oligonucleotides with fluorophores (1), (2), (3), (4), (5) and (6).** The required mass of *N*-hydroxysuccinimide ester (NHS) was calculated, considering a molar excess of 8 equivalents of NHS ester: mass of NHS ester [mg] = 8 × mass of modified oligonucleotide [mg] × molar mass of NHS ester [g/mol]/molar mass of modified oligonucleotide [g/mol]. The total volume of the reaction mixture was determined, considering the final concentration of 200 μM. The NHS ester was dissolved in 1/10 of the total reaction volume, in DMSO, and then mixed with the modified oligonucleotide in 9/10 of the total reaction volume in 0.1 M sodium bicarbonate. The NHS ester was added to the modified oligonucleotide and thoroughly stirred for 1 min with the aid of a vortex. Then the reaction continued with stirring for 12 h on an orbital shaker at 20°C and protected from light. The conjugate was purified using the ethanol precipitation method. Then 1/10 of the volume of 3 M NaCl and 2.5 volumes of cold (−20°C) absolute ethanol were added to the reaction mixture. The mixture was thoroughly stirred with vortex and incubated for 30 min at −20°C. After incubation, the reaction mixture was centrifuged at 12000 *g* for 30 min and the supernatant removed by decantation. The obtained bioconjugate (pellet) was washed 4 times with 70% ethanol (4 × 1 mL) and then air-dried.

**RNA-FISH protocol.** Two microorganisms were selected as biological models: (i) yeast, *S. cerevisiae* and (ii) bacteria: *Bacillus* sp. from the culture collection of the Laboratory of Biodegradation and Biotechnology of the HERCULES Laboratory (University of Évora, Portugal).

Bacterial and yeast cells were initially cultured for a period of 2 days using nutrient agar containing (g/L): peptone—5.0, beef extract powder—3.0, and agar—15.0 (pH 7.4) and YPD-agar composed of (g/L): glucose—20.0, peptone—20.0, yeast extract—10.0, and agar—20.0 (pH 6.0). This culture was maintained at a temperature of 30°C and subsequently stored at 4°C. To prepare the inocula, cells were harvested from the fresh surfaces of the slants using 2.0 mL of physiological saline solution. Following this, Erlenmeyer flasks (250 mL) containing 100 mL of NB and YEPD were inoculated and then incubated at 30°C with continuous shaking at 120 rpm. Cells were collected during the exponential growth phases, which occurred 6 h after inoculation, and subsequently washed using PBS.

**RNA-FISH.** The RNA-FISH methodology consists of several preparatory steps, such as: (i) fixation of sample cells; (ii) cell permeabilization; (iii) hybridization with specific probes to detect the respective target sequences; (iv) washing to remove unbound probes; (v) detection and quantification [32].

*Preparation of the probe solution (oligonucleotide-labeling).* The products obtained (precipitate) from the labeling reaction between the oligonucleotides and the labels (probes) were resuspended in RNase free water to obtain solutions with a final concentration of 120 ng/μL.

*Cell attachment and permeabilization.* The microbial cultures of *S. cerevisiae* and *Bacillus* strains were previously prepared in liquid medium and centrifuged at 1600 *g* for 5 min at 4°C and 13000 *g* for 15 min at 4°C, respectively, discarding the supernatant. The cells were washed by addition of 3.0 mL of PBS 10×, and centrifuged under the same conditions, discarding the supernatant. Subsequently, the cells (pellet) were fixed and permeabilized by adding 2.0 mL of absolute ethanol and incubated at room temperature for 1 h. After incubation, 6.0 mL of PBS 10× was added. The cells resuspended in EtOH : PBS 10× (50 : 50) were stored in the freezer at −20.0°C.

The fixed yeast and bacterial cells were thawed and centrifuged at 1600 *g* for 5 min at 4°C and 13000 *g* for 15 min at 4°C, respectively, and their supernatant was discarded. They were then resuspended in 1.0 mL of PBS 10×. Subsequently, in a microtube, 10.0 μL of cell suspension was added to 990.0 μL of methylene blue, vortexed and incubated at room temperature for 15 min. The crowned cells were counted in a Neubauer chamber, allowing the volume of the cell suspension to be calculated.

*Hybridization.* For hybridization, microtubes were prepared with identical aliquots containing $10^6$ yeast or $10^8$ bacterial cells fixed previously. After centrifugation at 1600 *g* for 5 min at 4°C (yeast cells) and 13000 *g* for 15 min at 4°C (bacterial cells), 80 μL of hybridization buffer-HB (0.9 M NaCl, 20 mM Tris-HCl, 0.1% SDS, pH 7.2) was added. The volume (2.0 μL of yeast and 20 μL of bacteria) of the corresponding RNA-FISH probe stock solution (120 ng/μL) was then added to each FISH assay. The samples were shaken and incubated in a water bath at 46°C for 2 h. The FISH assays carried out were as follows: (i) a blank without added probe, (ii) controls for natural autofluorescence and FISH-induced autofluorescence, (iii) controls with added EUK516-(**1**), EUK516-(**2**), EUK516-(**3**), EUK516-(**4**), EUK516-(**5**) and EUK516-(**6**) (universal probes for eukaryotes, being the positive control for yeast), EUB338-(**1**), EUB338-(**2**), EUB338-(**3**), EUB338-(**4**), EUB338-(**5**) and EUB338-(**6**) (universal probes for bacteria, being the positive control for bacteria and the negative control for yeast).

*Washing.* After hybridization, cells were washed with HB (100 μL) and incubated in a water bath (46°C, 30 min). Finally, after centrifugation at 1600 *g* for 5 min at 4°C (yeast cells) and 13000 *g* for 15 min at

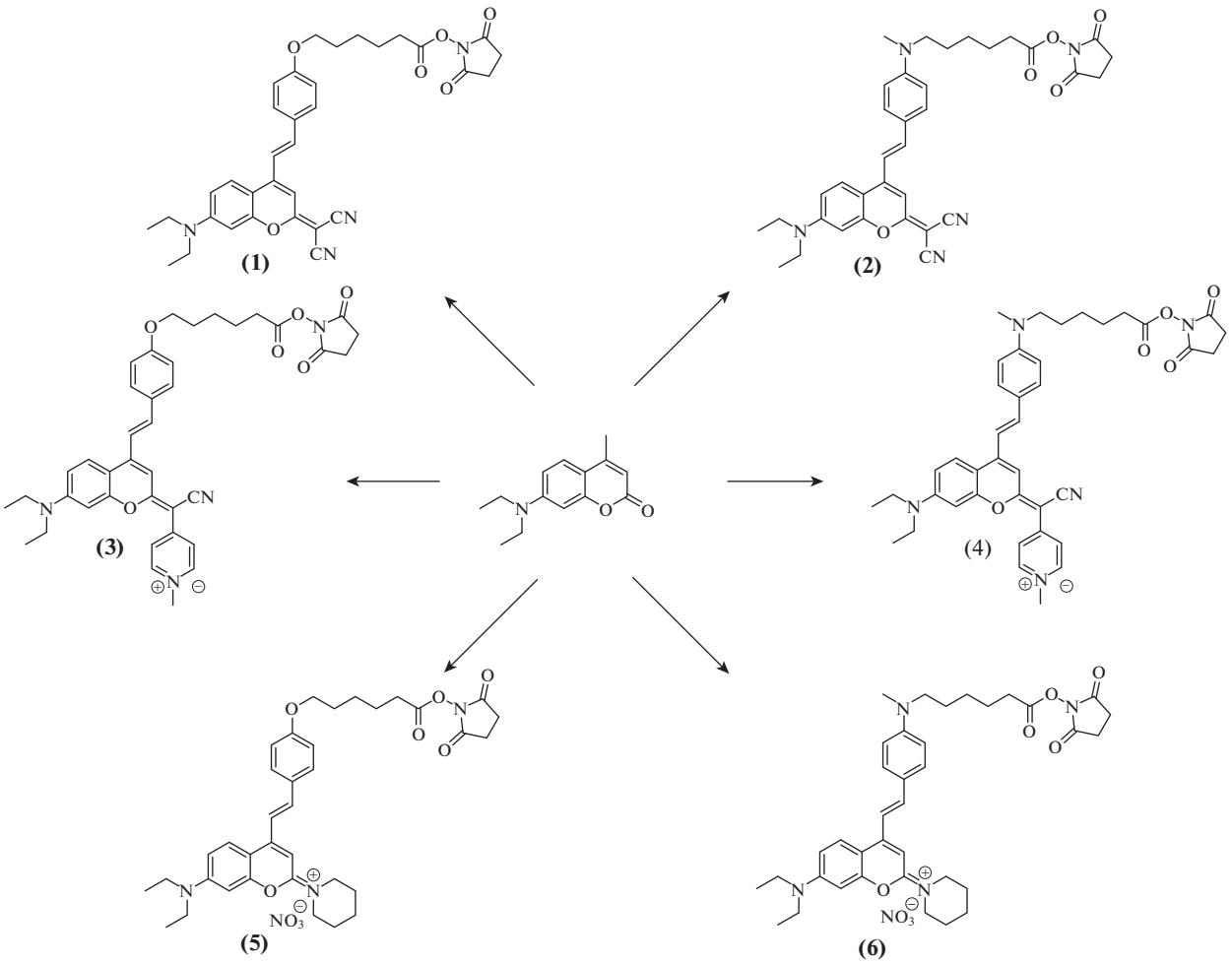


**Fig. 1.** Structure of the synthesized fluorescent labels.

4°C (bacterial cells), cells were resuspended in 400 µL of PBS 10×. Samples were analyzed by epifluorescence microscopy (EM) and flow cytometry (FC) according to the procedure described by Branco et al. [33].

**The EM and FC analysis.** For conducting microscopic analysis, we applied small portions of the samples onto microscope slides. These samples were then examined using an epifluorescence microscope (BA410E Motic model equipped with a 100W quartz halogen Koehler illumination system featuring intensity control and an epi-attachment EF-UPR-III, along with a power supply unit MXH-100, all from Motic in Spain).To facilitate this analysis, we utilized Motic filters designed for TRITC (excitation wavelength: 540/40×; dichroic mirror: 565DCLP; barrier filter: 605/55 m) and FITC (excitation wavelength: 480/40×; dichroic mirror: 505DCLP; barrier filter: 535/40 m) fluorescence. We captured microphotographs using a Moticam PRO 282B camera connected to the microscope and subsequently visualized the images using Motic Images Plus 2.0$^{LM}$ software (Motic, Spain).

Muse® Cell Analyzer and MuseSoft 1.4.0.0 software were used for the FC analysis. For each RNA-FISH assay the percentage of cells that become fluorescent after FISH treatment and their fluorescence intensities (FI), using the red (680/30) photodiode detector, were analyzed. To perform this, 1000 events were acquired. FI values were recorded on a gate that was first defined in FI-versus- Forward Scatter (FSC) density plot considering the results of the blanks, controls, and test assays. The probe-conferred fluorescence intensity (FIpro), i.e. summation of the fluorescence intensities of cells detected after RNA-FISH treatment using any of the probes tested (EUB338- or EUK516-), was directly calculated from the results given by the flow cytometer. Each sample was run in triplicate.

## RESULTS AND DISCUSSION

In this research, the potential of the 4-styrylcoumarin derivative labels synthesized using the 7-diethylamino-4-methylcoumarin as a cost-effective starting material was evaluated (Fig. 1), as they show

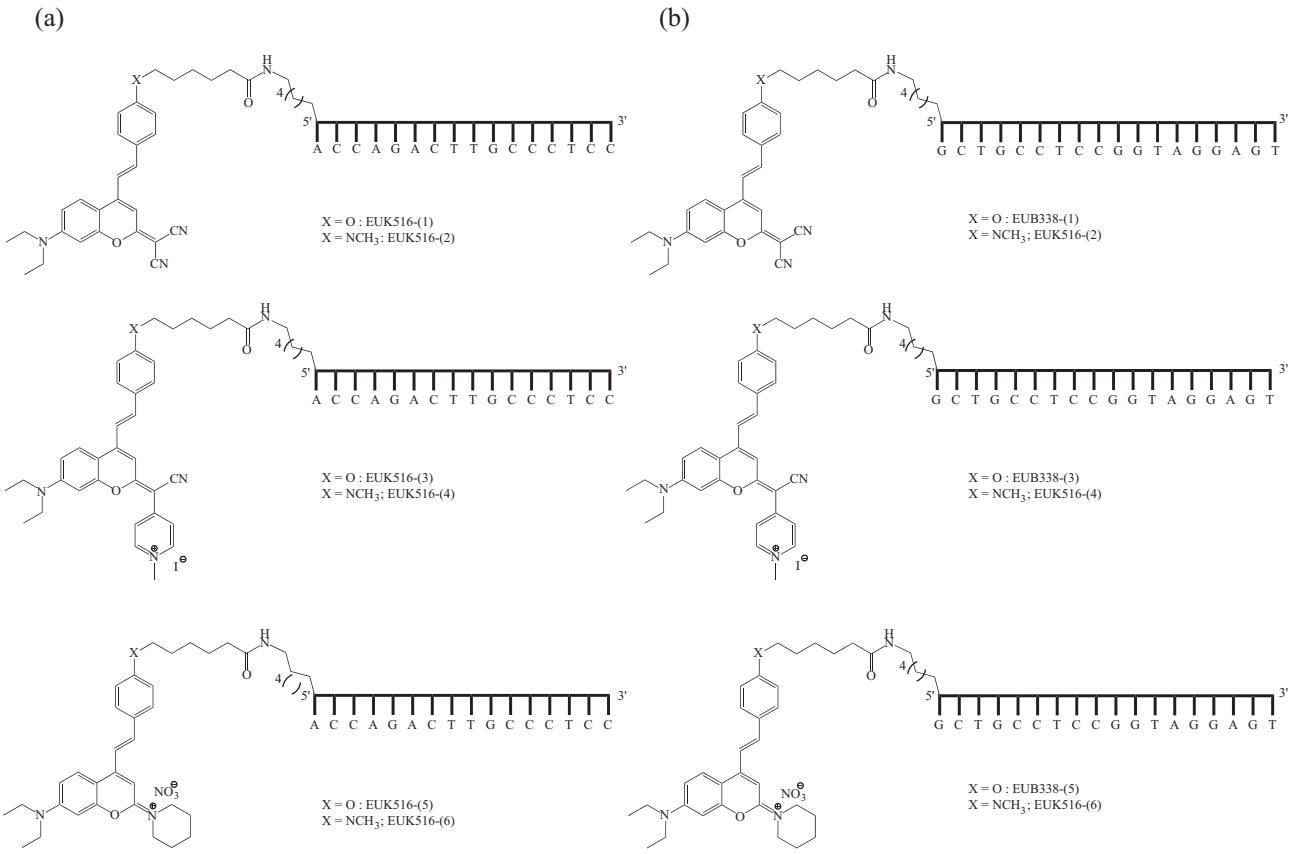


**Fig. 2.** Fluorescent oligonucleotide probes: (a) Oligonucleotide probes complementary to eukaryotic cell RNA; (b) oligonucleotide probes complementary to prokaryotic cell RNA.

promise as effective fluorescent labels for biomolecules. The 5'-AC6 amino-modified oligonucleotide sequences used for the development of these newly fluorescent probes were EUK516-mod (5'-ACCAGACTTGCCCTCC-3') and EUB338-mod (5'-GCTGCCTCCCGTAGGAGT-3'). These oligonucleotide sequences target the rRNA regions of eukaryotic and prokaryotic cells, respectively. The performance of these probes was evaluated on microorganisms sourced from the culture collection at the Laboratory of Biodegradation and Biotechnology within the HERCULES Laboratory at the University of Évora, Portugal. The probes demonstrated high efficacy when used as RNA-FISH probes. The methodology used to generate these fluorescent probes was derived from well-established experimental protocols outlined in existing literature [32]. This methodology involves chemically labeling oligonucleotides with fluorescent labels, creating a covalent bond between the fluorescent labels (1, 2, 3, 4, 5, and 6) and commercially available 5'-AC6 amino-modified oligonucleotide sequences (EUK516-mod or EUB338-mod) via the amino group situated at the 5'-terminus. It's important to highlight that introducing 6 carbon spacers for connecting the fluorescent labels to the oligonucleotides offered several benefits. Firstly, it heightened the fluorescence signal intensity when compared to probes with direct conjugation. Additionally, it eased the interaction between the fluorescent labels and oligonucleotide sequences by minimizing steric hindrance. Six of these new probes were designed to target the rRNA region of eukaryotic cells designated as EUK516-(**1**), EUK516-(**2**), EUK516-(**3**), EUK516-(**4**), EUK516-(**5**), and EUK516-(**6**), while the remaining 6 probes were tailored for the rRNA region of prokaryotic cells labeled as EUB338-(**1**), EUB338-(**2**), EUB338-(**3**), EUB338-(**4**), EUB338-(**5**), and EUB338-(**6**) (Fig. 2).

**Hybridization of *S. cerevisiae* cells.** The results obtained by flow cytometry of the hybridization of *S. cerevisiae* cells with commercial and synthesized oligonucleotide probes are shown in Fig. 3. After a thorough examination of these results, it is evident that yeast cells, when labeled with EUK516 oligonucleotide probes, exhibit significantly higher fluorescence compared to autofluorescence. This outcome aligns with expectations, as these probes specifically target the rRNA region of eukaryotic cells (Figs. 3a, 3c, 3e, 3g, 3i, 3k and 3m).

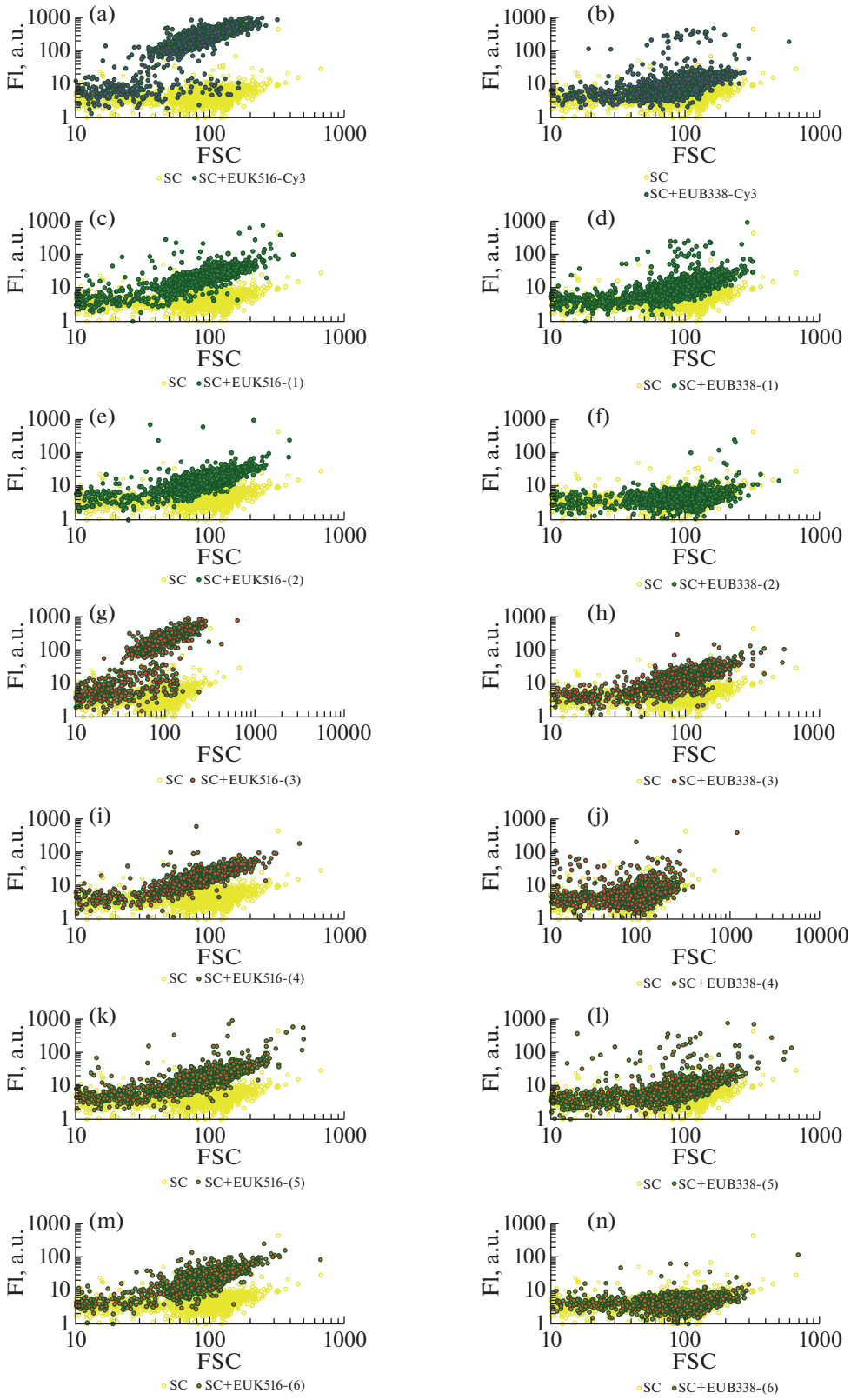


**Fig. 3.** Flow cytometry (FC) results (fluorescence intensity (FI)/forward scattering (FSC)) referring to the hybridization assays of *S. cerevisiae* cells (SC) with the oligonucleotide probes: (a) EUK516-Cy3; (b) EUB338-Cy3; (c) EUK516-(**1**); (d) EUB338-(**1**); (e) EUK516-(**2**); (f) EUB338-(**2**); (g) EUK516-(**3**); (h) EUB338-(**3**); (i) EUK516-(**4**); (j) EUB338-(**4**); (k) EUK516-(**5**); (l) EUB338-(**5**); (m) EUK516-(**6**); (n) EUB338-(**6**).

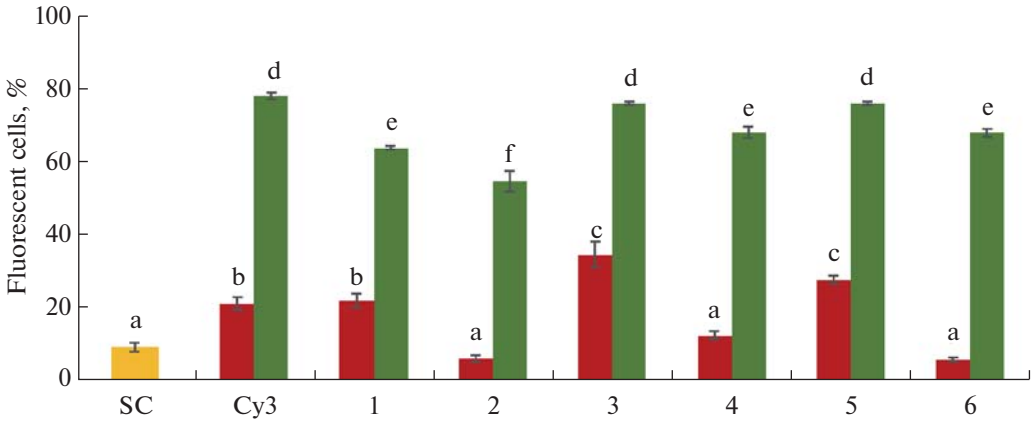


**Fig. 4.** Percentage of the fluorescent *S. cerevisiae* cells (SC) labeled with EUK516 (red) and EUB338 (green) probes with different markers (**1**, **2**, **3**, **4**, **5**, **6** and Cy3) and their respective blank. In each assay, 1000 cells were analyzed in triplicate. Values correspond to the average of flow cytometry measurements and error bars to standard deviation (± SD). In each plot, different letters located over the error bars indicate significant differences ($p < 0.05$).

Cells that underwent hybridization with the EUK516-Cy3 probe exhibited significantly higher fluorescence intensity in comparison to the intrinsic autofluorescence of unmarked yeast cells (Fig. 3a). This robust fluorescence signal indicated successful hybridization of the EUK516-Cy3 probe, demonstrating its effective binding rates. In contrast, cells exposed to the EUB338-Cy3 probe emitted fluorescence signals comparable to the autofluorescence exhibited by unmarked cells, as anticipated, indicating the absence of hybridization (Fig. 3b). Thus, this probe serves its intended purpose as a negative control in experiments involving eukaryotic cells, confirming that under the experimental conditions cell autofluorescence provides specific and reliable detection. For cells hybridized with the EUK516 probes with the synthesized labels, cells labeled with the EUK516-(**1**), EUK516-(**2**), EUK516-(**3**), EUK516-(**4**), EUK516-(**5**), EUK516-(**6**) probes showed fluorescence signals (Figs. 3c, 3e, 3g, 3i, 3k and 3m). Cells that underwent hybridization with EUB338 probes labeled as EUB338-(**1**), EUB338-(**2**), EUB338-(**3**), EUB338-(**4**), EUB338-(**5**), and EUB338-(**6**) produced fluorescence signals indistinguishable from the autofluorescence of yeast cells (Figs. 3d, 3f, 3h, 3j, 3l and 3n).

**Percentage of fluorescent cells from *S. cerevisiae*.** *S. cerevisiae* cells hybridized with the synthesized oligonucleotide probes EUK516-(**3**) and EUK516-(**5**) showed percentage values of fluorescent cells significantly identical to those of cells hybridized with the commercial probe EUK516-Cy3 (Fig. 4). These results affirm the high specificity of these probes for labeling the *S. cerevisiae* cells. Conversely, cells hybridized with probes EUK516-(**1**), EUK516-(**4**), and EUK516-(**6**) exhibited a substantial percentage of fluorescent cells, ranging from 64.7 to 67.9%, which closely resembled the values observed with the commercial probe. These findings underscore the efficacy of this custom probe for specifically labeling *S. cerevisiae* cells. Additionally, although cells subjected to hybridization with EUK516-(**2**) probes displayed lower percentages of fluorescent cells, they still demonstrated commendable specificity in labeling yeast cells.

**Results obtained by epifluorescence microscopy.** Figure 5 presents the epifluorescence microscopy outcomes from hybridization assays involving *S. cerevisiae* cells with commercial and synthesized oligonucleotide probes. The results from fluorescence microscopy aligned with the data generated through flow cytometry, confirming that within the image in Figs. 5a, 5c, 5e, 5g, 5i, 5k, and 5m), the oligonucleotide probes EUK516-Cy3, EUK516-(**1**), EUK516-(**2**), EUK516-(**3**), EUK516-(**4**), EUK516-(**5**), and EUK516-(**6**) exhibit more pronounced signals of intensity. However, in the context of hybridization assays involving *S. cerevisiae* cells with the EUB338 oligonucleotide probes, no discernible fluorescence signal could be observed (Figs. 5b, 5d, 5f, 5h, 5j, 5l and 5n).

**Hybridization of *Bacillus* cells.** The results from flow cytometry depicting the hybridization of the *Bacillus* cells with both commercial and synthesized oligonucleotide probes are displayed in Fig. 6. Upon analysis, it is evident that bacterial cells generally exhibit a higher level of fluorescence compared to autofluorescence when labeled with the EUB338 oligonucleotide probes. This is attributed to the targeting of the RNAr region specific to prokaryotic cells by these probes (Figs. 6c, 6e, 6g, 6i, 6k, and 6m). Particularly noteworthy is the observation that cells subjected to hybridization with the EUB338-Cy3 probe emitted significantly higher fluorescence intensity (FI) than untreated bacterial cells (Fig. 6a). In the case, cells hybridized with the EUB338-(**1**), EUB338-(**2**),

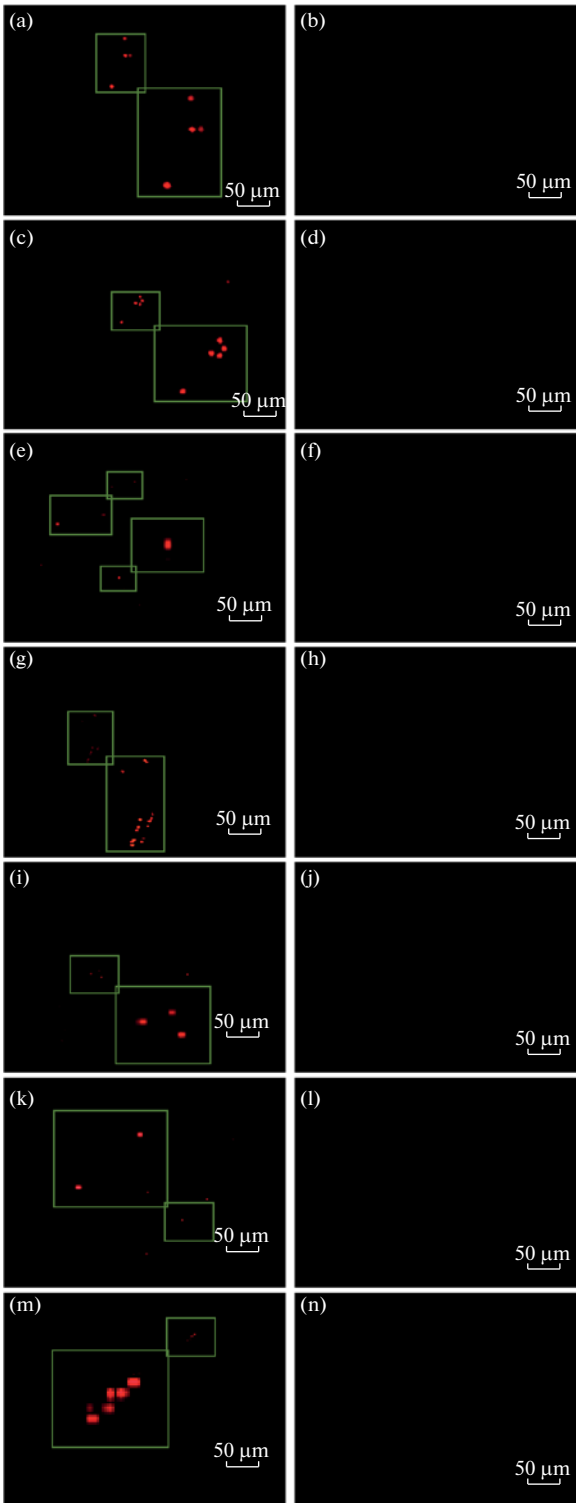


**Fig. 5.** Microphotographs obtained through epifluorescence microscopy in objective amplification of 50X with the TRITC filter referring to the hybridization assays of *S. cerevisiae* cells with the oligonucleotide probes: (a) EUK516-Cy3; (b) EUB338-Cy3; (c) EUK516-(**1**); (d) EUB338-(**1**); (e) EUK516-(**2**); (f) EUB338-(**2**); (g) EUK516-(**3**); (h) EUB338-(**3**); (i) EUK516-(**4**); (j) EUB338-(**4**); (k) EUK516-(**5**); (l) EUB338-(**5**); (m) EUK516-(**6**); (n) EUB338-(**6**).

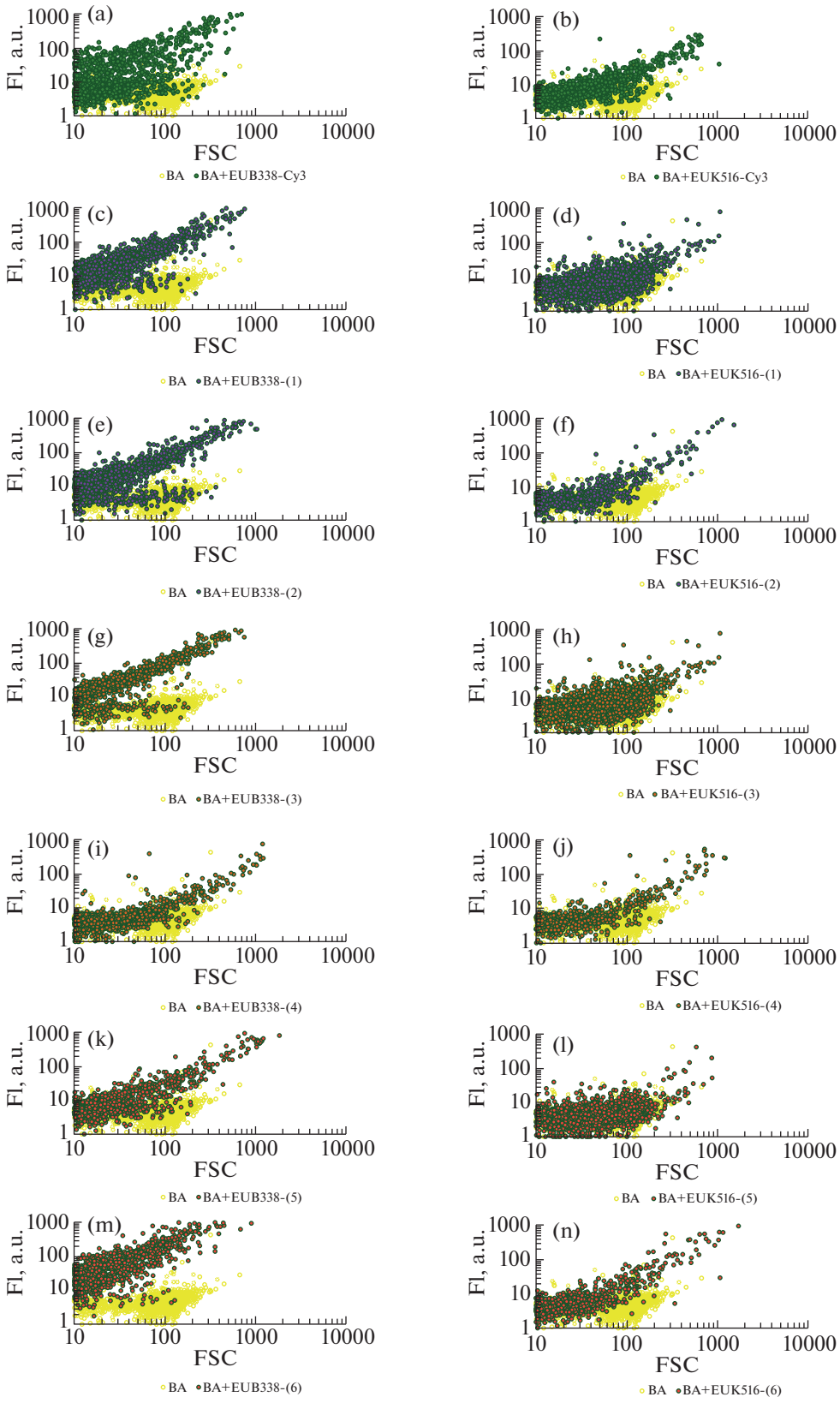


**Fig. 6.** Flow cytometry (FC) results (fluorescence intensity (FI)/forward scattering (FSC)) referring to the hybridization assays of *Bacillus* cells (BA) with the oligonucleotide probes: (a) EUB338-Cy3; (b) EUK516-Cy3; (c) EUB338-(**1**); (d) EUK516-(**1**); (e) EUB338-(**2**); (f) EUK516-(**2**); (g) EUB338-(**3**); (h) EUK516-(**3**); (i) EUB338-(**4**); (j) EUK516-(**4**); (k) EUB338-(**5**); (l) EUK516-(**5**); (m) EUB338-(**6**); (n) EUK516-(**6**).

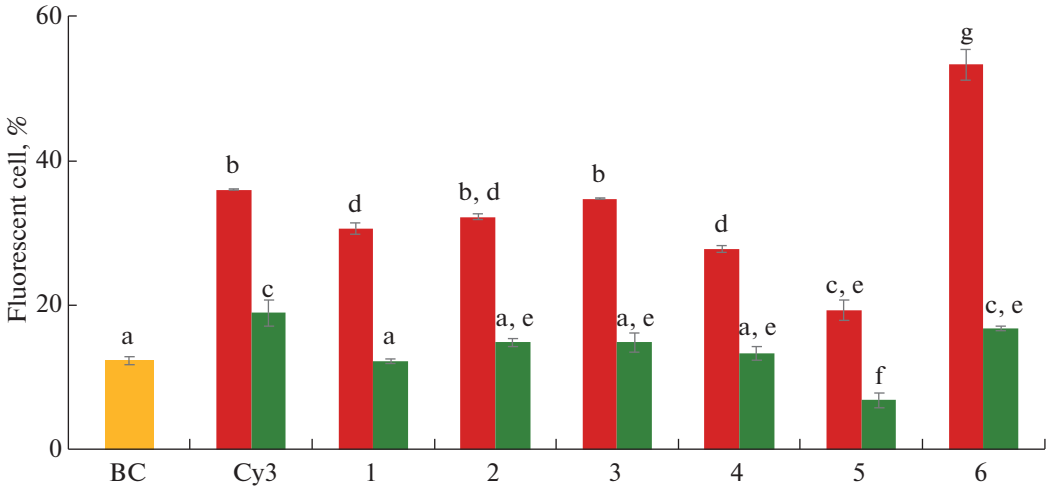


**Fig. 7.** Percentage of the fluorescent *Bacillus* cells labeled with EUK516 (green) and EUB338 (red) probes with different markers (**1**, **2**, **3**, **4**, **5**, **6** and Cy3) and their respective blank. In each assay, 1000 cells were analyzed in triplicate. Values correspond to the average of flow cytometry measurements and error bars to standard deviation (± SD). In each plot, different letters located over the error bars indicate significant differences ($p < 0.05$).

EUB338-(**3**), EUB338-(**4**), EUB338-(**5**) and EUB338-(**6**) probes exhibited fluorescence intensities (FI) surpassing those of untreated bacterial cells, indicating a clear enhancement in fluorescence levels (Figs. 6d, 6f, 6h, 6j, 6l and 6n).

**Percentage of the fluorescent *Bacillus* cells.** The hybridization of *Bacillus* cells with the synthesized oligonucleotide probes EUB338-(**1**), EUB338-(**2**), EUB338-(**3**), EUB338-(**4**), EUB338-(**5**), and EUB338-(**6**) resulted in a notable increase in the percentage of fluorescent cells compared to unlabeled cells (Fig. 7). Specifically, when *Bacillus* cells were subjected to hybridization with the custom-synthesized oligonucleotide probe EUB338-(**6**), there was a statistically significant increase in the percentage of fluorescent cells ($p < 0.05$) compared to cells hybridized with the commercially available probe EUB338-Cy3. These results strongly indicate the exceptional specificity of EUB338-(**6**) for labeling bacterial cells. Similarly, the probes EUB338-(**2**) and EUB338-(**3**) also exhibit comparable percentages of fluorescent cells to the commercial EUB338-Cy3 probe, further confirming their high specificity for labeling *Bacillus* cells. On the contrary, EUB338-(**1**) and EUB338-(**4**) probes, although displaying reduced fluorescence intensity compared to cells hybridized with EUB338-Cy3, demonstrated relatively high percentages of fluorescent cells, approaching the levels observed with the commercial probe. In contrast, cells treated with the EUB338-(**5**) probe exhibited a significantly lower percentage of fluorescent cells, suggesting its limited specificity for labeling these cells.

**Results obtained by epifluorescence microscopy.** Figure 8 displays the outcomes obtained through epifluorescence microscopy for *Bacillus* hybridization assays employing both commercial and synthesized oligonucleotide probes. Fluorescence microscopy observations validate the findings derived from flow cytometry, as the oligonucleotide probes EUB338-Cy3, EUB338-(**1**), EUB338-(**2**), EUB338-(**3**), EUB338-(**4**), EUB338-(**5**), and EUB338-(**6**) (Figs. 8a, 8c, 8e, 8g, 8i, 8k, and 8m) exhibited higher fluorescence intensities. Conversely, in the case of *Bacillus* hybridization assays with the probes EUK516-Cy3, EUK516-(**1**), EUK516-(**2**), EUK516-(**3**), EUK516-(**4**), EUK516-(**5**), and EUK516-(**6**), no fluorescence signal was detected, as anticipated (Figs. 8b, 8d, 8f, 8h, 8j, 8l, and 8n). These results confirm once again that these probes lack specificity for prokaryotic cells, reinforcing the selective binding of the synthesized fluorophores to the respective oligonucleotide probes, without establishing non-specific bonds with the cells.

**Photophysical properties.** Photophysical properties of the synthesized 4-styrylcoumarin derivative labels, namely their absorption and emission properties, as well as fluorescence quantum yields, are summarized in Table 1. The percentage of fluorescently labeled *S. cerevisiae* cells with EUK516-(**1**), EUK516-(**3**), and EUK516-(**5**) exceeded that of cells labeled with EUK516-(**2**), EUK516-(**4**), and EUK516-(**6**) (Fig. 4). These findings suggest that the probes with the highest quantum yields correspond to those displaying the highest percentage of fluorescent cells. ($\Phi_F$ (EUK516-(**1**)) = 0.29, $\Phi_F$ (EUK516-(**3**)) = 0.10 and $\Phi_F$ (EUK516-(**5**)) = 0.92) (Table 1).

According to the results obtained in this study, it was concluded that:

(i) the fluorescent 4-styrylcoumarin derivative labels serve as suitable components for tagging biomolecules containing primary amine groups. Specifi-

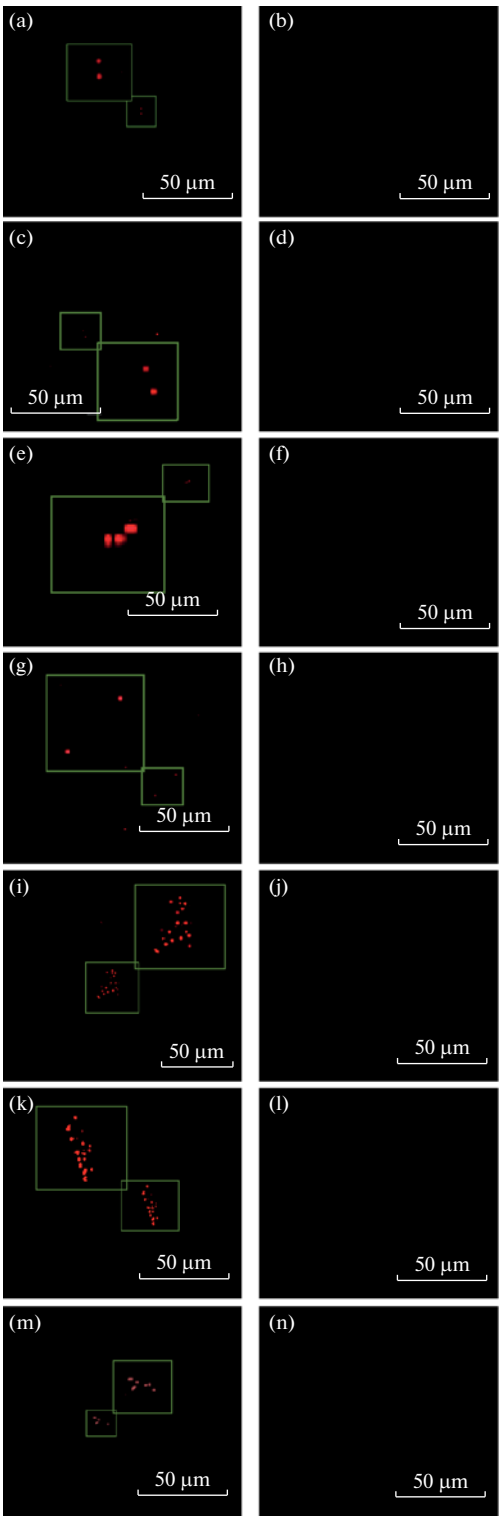


**Fig. 8.** Microphotographs obtained through epifluorescence microscopy in objective amplification of 100 X with the TRITC filter referring to the hybridization assays of *Bacillus* cells with the oligonucleotide probes: (a) EUB338-Cy3; (b) EUK516-Cy3; (c) EUB338-(**1**); (d) EUK516-(**1**); (e) EUB338-(**2**); (f) EUK516-(**2**); (g) EUB338-(**3**); (h) EUK516-(**3**); (i) EUB338-(**4**); (j) EUK516-(**4**); (k) EUB338-(**5**); (l) EUK516-(**5**); (m) EUB338-(**6**); (n) EUK516-(**6**).

**Table 1.** Spectroscopic properties of 7-diethylamino-4-methylcomarin derivatives

| Compound | $\lambda_{abs}$[a], nm | $\lambda_{em}$[b], nm | Stokes shift, nm, $cm^{-1}$ | $\varepsilon$[c], $cm^{-1}\ M^{-1}$ | $\Phi_F$[d] |
|---|---|---|---|---|---|
| 1 | 523 | 597 | 74, 2370 | 24000 | 0.29 |
| 2 | 498 (576) | 624 | 126, 4055 | 59000 | 0.27 |
| 3 | 589 (615) | 663 | 74, 1895 | 55000 | 0.10 |
| 4 | 634 | 683 | 49, 1132 | 113500 | 0.07 |
| 5 | 404 | 577 | 173, 7421 | 30000 | 0.92 |
| 6 | 487 | 628 | 141, 4610 | 64000 | 0.56 |

[a] Absorption maxima in acetonitrile. [b] Emission maxima in acetonitrile. [c] Molar extinction coefficient at longest wavelength transition. [d] Fluorescence quantum yield in ethanol, determined using 7-diethylamino-4-methymcoumarin ($\Phi_F = 0.73$ in ethanol) as a standard.

cally, they demonstrate remarkable effectiveness in producing single-fluorescent-labeled oligonucleotides that incorporate amino-modified nucleotides with high yields;

(ii) the resulting fluorescent oligonucleotide probes demonstrated high efficacy as RNA-FISH probes, enabling the specific detection of microbial cells. These findings lay the groundwork for exploring numerous other potential applications for these amino-reactive fluorescent labels;

(iii) the proportion of fluorescent cells in the bacterial cell probes exhibited a notable decrease when compared to the probes used with yeast cells;

(iv) several of the synthesized probes exhibited a proportion of fluorescent cells that matched or exceeded that of the commercial fluorescent label (Cy3). This highlights their exceptional effectiveness as RNA-FISH probes, enabling the precise identification of microbial cells.

## FUNDING

The authors acknowledge financial support to FCT—Foundation for Science and Technology, I.P.—within the scope of the projects UIDB/04449/2020 (HERCULES Lab), UIDB/04033/2020 (CITAB), ART3mis (2022.07303.PTDC/FCT) and the Old Goa Revelations project (2022.10305.PTDC/FCT) and also through the Ph.D. Grant UI/BD/153584/2022 (R.E.). The authors additionally acknowledge the City University of Macau endowment to the Sustainable Heritage Chair and Sino-Portugal Joint Laboratory of Cultural Heritage Conservation Science, supported by the Belt and Road Initiative.

## ETHICS APPROVAL AND CONSENT TO PARTICIPATE

This work does not contain any studies involving human and animal subjects.

## CONFLICT OF INTEREST

The authors of this work declare that they have no conflicts of interest.

## REFERENCES

1. Sednev, M.V., Belo, V.N., and Hell, S.W., *Methods Appl. Fluoresc.*, 2015, vol. 3, no. 4, p. 042004. https://doi.org/10.1088/2050-6120/3/4/042004
2. Giepmans, B., Adams, S., Ellisman, M., and Tsien, R. *Science*, 2006, vol. 312, pp. 217–224. https://doi.org/10.1126/science.1124618
3. Dirks, R.W. and Tanke, H.J., *BioTechniques*, 2006, vol. 40, no. 4, pp. 489–495. https://doi.org/10.2144/000112121
4. Maekawa, M. and Fairn, G.D., *J. Cell Sci.*, 2014, vol. 127, no. 15, pp. 4801–4812. https://doi.org/10.1242/jcs.150524
5. Chen, J., Liu, W., Zhou, B., Niu, G., Zhang, H., Wu, J., et al., *J. Org. Chem.*, 2013, vol. 78, no. 12, pp. 6121–6130. https://doi.org/10.1021/jo400783x
6. Hanson, G. and Hanson, B., *Comb. Chem. High T. SCR.*, 2008, vol. 11, no. 7, pp. 505–513. https://doi.org/10.2174/138620708785204090
7. Maurel, D., Comps-Agrar, L., Brock, C., Rives, M., Bourrier, E., Ayoub, M., et al., J., *Nat. Methods*, 2008, vol. 5, no. 6, pp. 561–567. https://doi.org/10.1038/nmeth.1213
8. Yin, J., Straight, P., McLoughlin, S., Zhou, Z., Lin, A., Golan, D., et al., *Proc. Natl. Acad. Sci. U. S. A.*, 2005, vol. 102, no. 44, pp. 15815–15820. https://doi.org/10.1073/pnas.0507705102
9. Sahoo, H., *RSC Adv.*, 2012, vol. 2, no. 18, pp. 7017–7029. https://doi.org/10.1039/C2RA20389H
10. Hermanson T., *Bioconjugate Techniques,* London: Elsevier, 2013, 3 ed. ISBN: 9780123822390.
11. *Phytochemicals in Human Health, IntechOpen Publications*, London: UK, 2019, vol. 1, chapter 8. https://doi.org/10.5772/intechopen.85973

12. Fang, X., Zheng, Y., Duan, Y., Liu, Y., and Zhong, W., *Anal. Chem.*, 2019, vol. 91, no. 1, pp. 482–504. https://doi.org/10.1021/acs.analchem.8b05303
13. Kobayashi, H., Ogawa, M., Alford, R., Choyke, P., and Urano, Y., *Chem. Rev.*, 2010, vol. 110, no. 5, pp. 2620–2640. https://doi.org/10.1021/cr900263j
14. Gall, J. G. and Pardue, M.L., *Proc. Natl. Acad. Sci. U. S. A.*, 1969, vol. 63, no. 2, pp. 378–383. https://doi.org/10.1073/pnas.63.2.378
15. John, H.A., Birnstiel, M.L., and Jones, K.W., *Nature,* 1969, vol. 223, no. 5206, pp. 582–587.
16. Amann, R. and Moraru, C., *Syst. Appl. Microbiol.*, 2012, vol. 35, no. 8, pp. 483–484. https://doi.org/10.1016/j.syapm.2012.10.002
17. Bauman, J.G., Wiegant, J., Borst, P., and Duijn, P.V., *Exp. Cell Res.*, 1980, vol. 128, no. 2, pp. 485–490. https://doi.org/10.1016/0014-4827(80)90087-7
18. Ballard, S.G. and Ward, D.C., *J. Histochem. Cytochem.*, 1993, vol. 41, no. 12, 1755–1759. https://doi.org/10.1177/41.12.8245423
19. Ren, T.B., Xu, W., Zhang, W., Zhang, X.X., Wang, Z.Y., Xiang, Z., et al., *J. Am. Chem. Soc.*, 2018, vol. 140, no. 24, pp. 7716–7722. https://doi.org/10.1021/jacs.8b04404
20. Liu, X., Xu, Z., and Cole, J.M., *J. Phys. Chem. C*, 2013, vol. 117, no. 32, pp. 16584–16595. https://doi.org/10.1021/jp404170w
21. Barot, K.P., Jain, S.V., Kremer, L., Singh, S., and Ghate, M.D., *Med. Chem. Res.*, 2015, vol. 24, pp. 2771–2798. https://doi.org/10.1007/s00044-015-1350-8
22. Riveiro, M., De Kimpe, N., Moglioni, A., Vázquez, R., Monczor, F., Shayo, et al., *Curr. Med. Chem.*, 2010, vol. 17, no. 13, pp. 1325–1338. https://doi.org/10.2174/092986710790936284
23. Martins, S., Avó, J., Lima, J., Nogueira, J., Andrade, L., Mendes, A., et al., *J. Photochem. Photobiol.*, 2018, vol. 353, pp. 564–569. https://doi.org/10.1016/j.jphotochem.2017.12.018
24. Lanke, S.K. and Sekar, N., *J. Fluoresc.*, 2016, vol. 26, pp. 949–962. https://doi.org/10.1007/s10895-016-1783-6
25. Zhang, G., Zheng, H., Guo, M., Du, L., Liu, G., and Wang, P., *Appl. Surf. Sci.*, 2016, vol. 367, pp. 167–173. https://doi.org/10.1016/j.apsusc.2016.01.110
26. Zaorska, E., Konop, M., Ostaszewski, R., Koszelewski, D., and Ufnal, M., *Molecules*, 2018, vol. 23, no. 9, p. 2241. https://doi.org/10.3390/molecules23092241
27. Gandioso, A., Bresolí-Obach R., Nin-Hill, A., Bosch, M., Palau, M., Galindo, A., et al., *J. Org. Chem.*, 2018, vol. 83, no. 3, pp. 1185–1195. https://doi.org/10.1021/acs.joc.7b02660
28. Bojtár, M., Kormos, A., Kis-Petik, K., Kellermayer-and, M., and Kele, P., *Org. Lett.*, 2019, vol. 21, no. 23, pp. 9410–9414. https://doi.org/10.1021/acs.orglett.9b03624
29. Eustáquio, R., Ramalho, J.P.P., Caldeira, A.T., and Pereira, A., *Molecules*, 2022, vol. 27, no. 5, p. 1461. https://doi.org/10.3390/molecules27051461
30. Eustáquio, R., Ramalho, J.P.P., Caldeira, A.T., and Pereira, A., *Molecules,* 2023, vol. 28, no. 19, p. 6822. https://doi.org/10.3390/molecules28196822
31. Eustáquio, R., Ramalho, J.P.P., Caldeira, A.T., and Pereira, A., *RSC Adv.* 2022, vol. 12, no. 14, pp. 8477–8484. https://doi.org/10.1039/d2ra00716a
32. *Methods in Molecular Biology*, Fan, Y.S., Ed., New Jersey: Humana, 2002, vol. 204, pp. 41–49.
33. Branco, P., Candeias, A., Caldeira, A.T., and Gonzalez-Perez, M. *Int. J. Food Microbiol.* 2020, vol. 314, p. 108415. https://doi.org/10.1016/j.ijfoodmicro.2019.108415